Lack of Myoglobin Causes a Switch in Cardiac Substrate Selection

Ulrich Flögel,* Tim Laussmann,* Axel Gödecke, Nadine Abanador, Michael Schäfers, Christian Dominik Fingas, Sabine Metzger, Bodo Levkau, Christoph Jacoby, Jürgen Schrader

Abstract—Myoglobin is an important intracellular O_2 binding hemoprotein in heart and skeletal muscle. Surprisingly, disruption of myoglobin in mice (myo$^{-/-}$) resulted in no obvious phenotype and normal cardiac function was suggested to be mediated by structural alterations that tend to steepen the oxygen pressure gradient from capillary to mitochondria. Here we report that lack of myoglobin causes a biochemical shift in cardiac substrate utilization from fatty acid to glucose oxidation. Proteome and gene expression analysis uncovered key enzymes of mitochondrial β-oxidation as well as the nuclear receptor PPARα to be downregulated in myoglobin-deficient hearts. Using FDG-PET we showed a substantially increased in vivo cardiac uptake of glucose in myo$^{-/-}$ mice (6.7±2.3 versus 0.8±0.5% of injected dose in wild-type, n=5, $P<0.001$), which was associated with an upregulation of the glucose transporter GLUT4. The metabolic switch was confirmed by ^{13}C NMR spetroscopic isotopomer studies of isolated hearts which revealed that [1,6-$^{13}C_2$]glucose utilization was increased in myo$^{-/-}$ hearts (38±8% versus 22±5% in wild-type, n=6, $P<0.05$), and concomitantly, [U-$^{13}C_{16}$]palmitate utilization was decreased in the myoglobin-deficient group (42±6% versus 63±11% in wild-type, n=6, $P<0.05$). Because of the O_2-sparing effect of glucose utilization, the observed shift in substrate metabolism benefits energy homoeostasis and therefore represents a molecular adaptation process allowing to compensate for lack of the cytosolic oxygen carrier myoglobin. Furthermore, our data suggest that an altered myoglobin level itself may be a critical determinant for substrate selection in the heart. The full text of this article is available online at http://circres.ahajournals.org. **(*Circ Res*. 2005;96:e68-e75.)**

Key Words: metabolism ■ β-oxidation ■ glucose ■ oxygen ■ heart

It is well known that red and white muscle are not only characterized by a largely different content of myoglobin (Mb), but also by significant differences in metabolism closely related to their physiological function.[1,2] Red muscles exhibit slow twitch speed, are fatigue resistant, and have an aerobic fat-, glucose-, and ketone-based metabolism. In contrast, white muscle fibers are fast contracting anaerobic fibers and easily fatigued because they have few respiratory proteins and metabolize glucose only as far as lactate. Similar to the red skeletal muscle, the heart has a high, enduring energy demand, which under normal conditions is primarily met by metabolism of fatty acids (FAs).[3] Nevertheless, in several cardiac diseases, such as ischemic cardiomyopathy, heart failure, hypertrophy, and dilated cardiomyopathy, a reduced oxidation of FAs and an enhanced glucose utilization has been found.[4] Interestingly, dilated and ischemic cardiomyopathies have also been reported to be accompanied by a decreased myocardial Mb content.[5] However, whether there is more then a mere correlation between muscle Mb level and substrate metabolism has not been explored so far.

In mice lacking Mb (myo$^{-/-}$), multiple compensatory mechanisms are induced that tend to steepen the oxygen pressure gradient to the mitochondria.[6–8] These include a higher capillary density, reduction in cell width, elevated hematocrit, increased coronary flow, and coronary flow reserve. However, substrate utilization was reported to be preserved in the absence of Mb, although in vitro, a modest increase in lactate utilization in the Mb mutant heart was noted.[8] To address the role of Mb in substrate selection of the heart in more detail, we utilized positron emission tomography (PET) using [^{18}F]fluorodeoxyglucose (FDG) and ^{13}C nuclear magnetic resonance (NMR) spectroscopy using [1,6-$^{13}C_2$]glucose and [U-$^{13}C_{16}$]palmitate to study cardiac intermediary metabolism in wild-type (WT) and Mb-deficient mice generated in our laboratory.[7] Furthermore, we analyzed the myocardial protein pattern of WT and myo$^{-/-}$ mice by 2-dimensional gel electrophoresis (2D-PAGE) and identified differentially expressed proteins by mass spectrometry. Additionally, we verified whether alterations at the protein level

Original received May 11, 2004; resubmission received March 3, 2005; revised resubmission received March 24, 2005; accepted March 28, 2005.

From the Institut für Herz-und Kreislaufphysiologie (U.F., T.L., A.G., N.A., C.D.F., C.J., J.S.), Heinrich-Heine-Universität Düsseldorf; Klinik und Poliklinik für Nuklearmedizin (M.S.), Universitätsklinikum Münster; Biomedizinisches Forschungszentrum (S.M.), Heinrich-Heine-Universität Düsseldorf; and Institut für Pathophysiologie, Zentrum für Innere Medizin (B.L.), Universitätsklinikum Essen, Germany.

*Both authors contributed equally to this work.

Correspondence to Dr Ulrich Flögel, Heinrich-Heine-Universität Düsseldorf, Universitätsstrasse 1, 40225 Düsseldorf, Germany. E-mail floegel@uni-duesseldorf.de

Circulation Research **is available at http://www.circresaha.org** **DOI: 10.1161/01.RES.0000165481.36288.d2**

are related to a gene regulatory switch. We found that similar to skeletal muscle, lack of Mb causes a switch in cardiac substrate selection from fatty acid to glucose utilization that is accompanied by a downregulation of key enzymes of the β-oxidation pathway.

Materials and Methods

Animals

Myo$^{-/-}$ mice were generated in our laboratory by deletion of the essential exon-2 via homologous recombination in embryonic stem cells as described previously.[7] Animal experiments were performed in accordance with the national guidelines on animal care and were approved by the local government. Before all metabolic experiments mice were fed with a standard chow diet and received tap water ad libitum.

Heart Perfusion for Metabolic Analysis

Preparation of murine hearts and retrograde perfusion at constant pressure of 100 mm Hg was performed essentially as described.[9] After hemodynamic and contractile parameters maintained constant under these conditions, hearts were finally switched to buffer containing 5 mmol/L [1,6-$^{13}C_2$]glucose, 0.5 mmol/L [U-$^{13}C_{16}$]palmitate (the latter bound to 3% essentially fatty acid free albumin; both from Cambridge Isotope Laboratories), and 50 μU insulin. After 25 minutes of perfusion, hearts were freeze-clamped, extracted with perchloric acid (PCA), neutralized, lyophilized, and stored at −20°C. A more detailed description of the heart perfusion protocol is provided in the expanded Materials and Methods section in the online data supplement available at http://circres.ahajournals.org.

Magnetic Resonance Measurements

Data were recorded on a Bruker DRX 9.4 Tesla WB NMR spectrometer operating at frequencies of 400.1 MHz for ^{1}H and 100.6 MHz for ^{13}C measurements.

Spectroscopy

Lyophilized PCA extracts were redissolved in 0.5 mL D_2O. Spectra were recorded from a 5-mm ^{1}H/^{13}C dual probe. Acquisition and processing parameters are given in detail in the online data supplement.

Isotopomer Analysis of Carbon Flow Into the Tricarboxylic Acid Cycle

The relative contributions of palmitate, glucose, and endogenous sources to the total acetyl-CoA pool entering the tricarboxylic acid (TCA) cycle were determined from isotopomer analysis of glutamate carbons C3 and C4. Consult the online data supplement for a detailed description of the analysis of ^{13}C NMR spectra.

Imaging

MRI was performed using a microimaging unit (Mini 0.5, Bruker) as described in the online data supplement.

High-Resolution PET

Myocardial glucose transport was noninvasively assessed in vivo by monitoring the uptake of FDG in intact mice, which before PET analysis had been functionally and morphologically characterized by MRI. Mice were anesthetized with isoflurane (1.5%) and kept at 37°C. Each mouse was injected with 10 MBq FDG in 100 μL 0.9% saline intravenously. After 60 minutes, mice were positioned on the bed of a submillimeter-resolution PET camera (quad-HIDAC, Oxford Positrons Ltd), and a 15-minute acquisition was initiated. Coronal images were then reconstructed (voxel size 0.25 mm^3, 0.7 mm full-width half-maximum). Myocardial FDG uptake was quantified by the ratio between myocardial radioactivity in a region-of-interest encompassing the left ventricular myocardium and the total injected dose (% injected dose, % ID).

Blood Serum

Determination of glucose, lactate, and fatty acids in blood serum was performed by the Central Laboratory of the University Hospital Düsseldorf using clinical routine protocols.

Proteome Analysis

Sample preparation and 2D-PAGE were essentially performed as previously reported[10] and a more detailed description is provided in the online data supplement. SDS-PAGE was performed on an ETTAN-DALT II vertical electrophoresis unit (Amersham Pharmacia Biotech). Equilibrated IPG strips were placed on top of the gel (size of 0.1×25.5×20 cm^3) and fixed in place by agarose sealing solution. Twelve gels were run simultaneously (settings: 30 minutes, 30 W; 4.5 hours, 180 W) and either silver-stained or stained by Coomassie blue R250. The gels were digitized and the obtained images analyzed as described in the online data supplement.

Protein Identification

Coomassie-stained spots were excised from preparative gels and analyzed by nano spray ESI-MS/MS using a SCIEX Q-STAR system (PE Sciex), as previously described.[10]

Expression Analysis

Expression levels were analyzed by real-time PCR using an ABI SDS 5700 real-time PCR analysis system on reverse-transcribed myocardial RNA isolated from 8 WT and myo$^{-/-}$ hearts, respectively. cDNA derived from 100 ng of total RNA was used for each reaction. Signals were amplified using the Taqman based assays on demand (ABI) for PPARα (Mm00440939_m1), short chain enoyl-CoA hydratase (Mm00659670_g1), and short chain acyl-CoA dehydrogenase (Mm00431617_m1) according to the suppliers instructions. Relative expression levels were determined by normalization to transferrin receptor (Mm00441941_m1) and TATA binding protein (Mm00446973_m1) as housekeeping genes.

Cell Fractionation and Western Analysis of GLUT4 Expression

Hearts were isolated from WT and myo$^{-/-}$ mice and separated into membranous and cytosolic fractions according to published procedures.[11] For Western analysis, 10 μg of membrane proteins and the corresponding volume fractions of the 30 000g supernatant were analyzed by Western blotting using a polyclonal rabbit anti-GLUT4 antibody (Abcam Ltd; 1:2500) followed by secondary HRPO-coupled goat anti-rabbit antibody (Sigma Heidelberg; 1:5000). Signals were detected by use of an ECL-kit (Amersham Biosciences).

Statistical Analysis

All results are expressed as mean±SD. For multiple comparisons, ANOVA followed by the Bonferroni correction was applied. A probability value of less than 0.05 was considered significant. The statistical analysis of the raw data from 2D-PAGE experiments was performed by the program "statistical analysis of microarrays, SAM."[12] The parameter "δ value" was adjusted in order to keep the number of false significant protein spots (90%) below 1. In a nonpaired t test, this translates to approximately $P<0.005$ for n=12. Additionally, changes in protein expression below 30% were considered to be of low biological relevance.

Results

^{13}C NMR Isotopomer Analysis

For analysis of the contribution of FA and glucose oxidation to TCA cycle turnover, isolated hearts paced at 500 bpm were perfused for 25 minutes with 5 mmol/L [1,6-$^{13}C_2$]glucose and 0.5 mmol/L [U-$^{13}C_{16}$]palmitate in the presence of 50 μU insulin. Under these conditions, left ventricular developed pressure was equal in both groups (114.4±9.8 mm Hg in WT versus 115.0±10.4 mm Hg in Mb-deficient hearts, n=8).

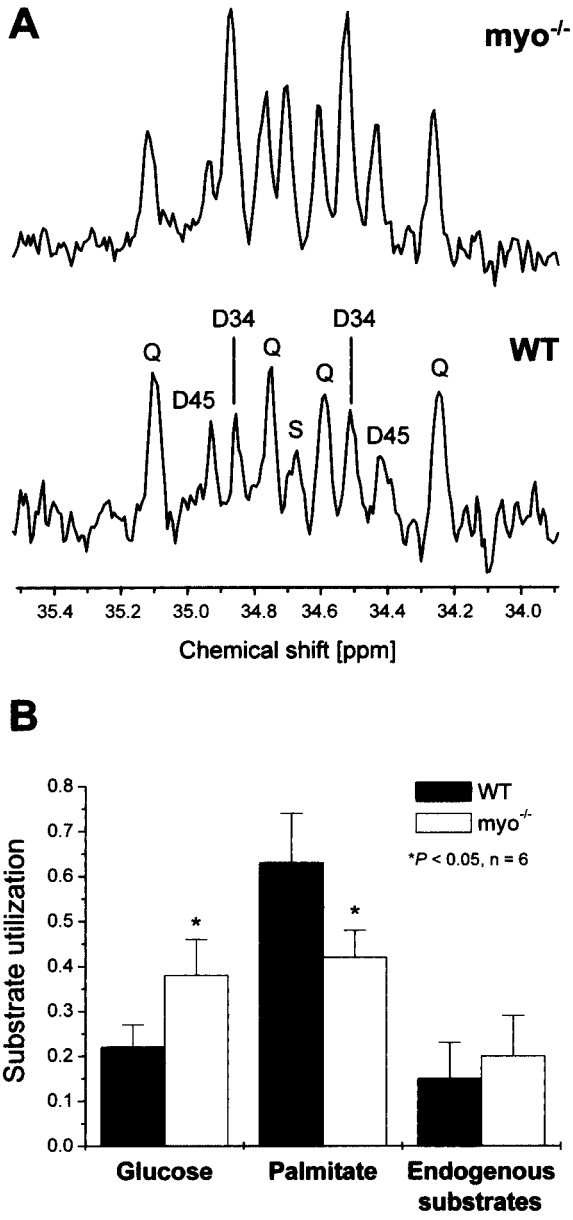

Figure 1. A, Representative sections of ^{13}C NMR spectra showing the glutamate C4 isotopomer pattern for WT and myo$^{-/-}$ PCA heart extracts. Hearts were perfused for 25 minutes with 5 mmol/L [1,6-$^{13}C_2$]glucose and 0.5 mmol/L [U-$^{13}C_{16}$]palmitate in the presence of 50 μU insulin. D34 indicates doublet because of J_{34} coupling (34 Hz); D45, doublet because of J_{45} coupling (51 Hz); Q, quartet (doublet of doublet) because of J_{345} coupling (J_{34} 34 Hz, J_{45} 51 Hz); S, singlet. B, Analysis of carbon flow into the TCA cycle in WT and myo$^{-/-}$ hearts under the conditions given above. Data are mean±SD (n=6, *P<0.05 vs WT). By definition, $F_{Palmitate}+F_{Glucose}+F_{Endogenous}=1$.

However, despite unrestricted cardiac function, we found myocardial oxygen consumption to be reduced by 7.5% in the transgenic group (15.63±1.43 μmol · min^{-1} · g^{-1} in WT versus 14.46±1.37 μmol · min^{-1} · g^{-1} in myo$^{-/-}$, n=8; P=0.09). High-resolution ^{13}C NMR spectra of the respective PCA extracts (Figure 1A) showed pronounced differences in the isotopomer pattern of the glutamate carbon C4 of WT (bottom) and myo$^{-/-}$ (top) hearts. The sum of the resonances (S+D34) reports the amount of acetyl-CoA derived from

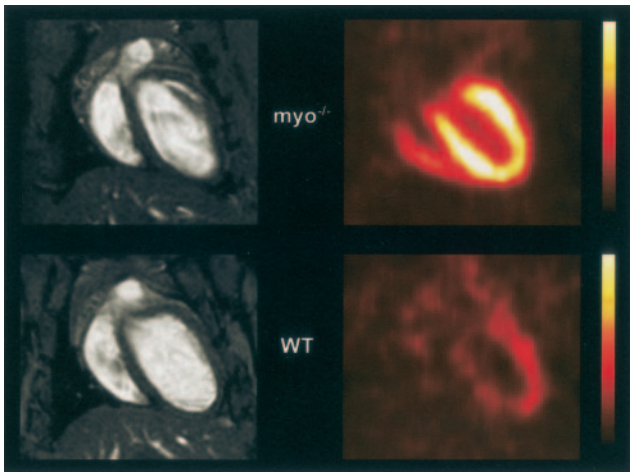

Figure 2. Matched noninvasive functional and metabolic imaging of WT (bottom) and myo$^{-/-}$ (top) mice in vivo. MRI (left panel, coronal slices) shows normal cardiac morphology and function (cf. online Table II) in WT and myo$^{-/-}$, whereas myocardial glucose uptake (right panel, matching coronal slices) measured by FDG-PET is markedly increased in myo$^{-/-}$ as compared with WT.

[1,6-^{13}C]glucose (entry of [2-^{13}C]acetyl-CoA into the TCA cycle), and the sum of (D45+Q) reflects the amount of acetyl-CoA derived from [U-$^{13}C_{16}$]palmitate (entry of [1,2-$^{13}C_2$]acetyl-CoA), irrespective of any cycling intermediate or pool sizes.[13] Thus, in the example shown in Figure 1A, it is obvious that in Mb-deficient hearts, the amount of carbons incorporated into glutamate that originate from glucose were increased whereas carbons originating from palmitate were decreased compared with WT hearts.

Quantitative analysis of the ^{13}C NMR spectra (Figure 1B) revealed that glucose utilization was significantly increased in myo$^{-/-}$ hearts (38±8% versus 22±5% in WT, n=6; P<0.05), and concomitantly, palmitate utilization was significantly decreased in the Mb-deficient group (42±6% versus 63±11% in WT, n=6; P<0.05), whereas the contribution of endogenous substrates (ie, glycogen or unlabeled glucose and FAs) was similar in both groups. Furthermore, no differences were observed in pool sizes of metabolites (cf. Table I in the online data supplement) and fractional enrichments (data not shown) of alanine, glutamate, and lactate between WT and myo$^{-/-}$ hearts.

In Vivo MRI and PET Analysis

In order to verify whether the enhanced glucose metabolization found in isolated perfused hearts of myo$^{-/-}$ mice can also be observed under in vivo conditions, myocardial glucose transport was noninvasively assessed by monitoring the uptake of FDG in intact mice. Before PET analysis, all mice were initially characterized by MRI, which showed similar values for diastolic and systolic volumes as well as cardiac output in both groups (Figure 2, left, and online Table II). Despite being morphologically and functionally undistinguishable, FDG-PET revealed significant differences between WT and myo$^{-/-}$ mice (Figure 2, right) in that myocardial FDG uptake was substantially enhanced in Mb-deficient

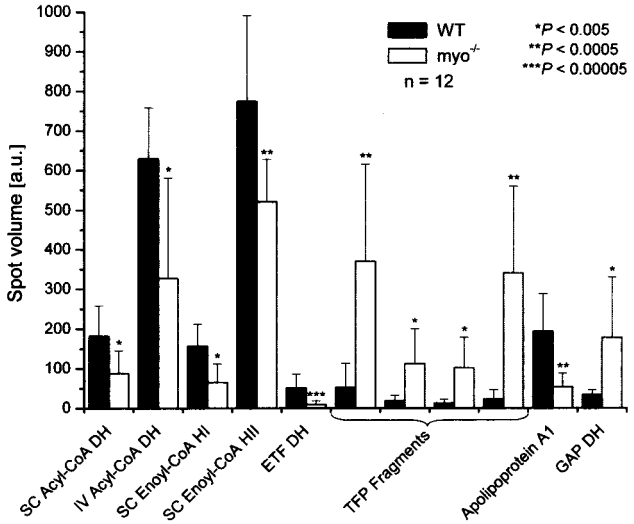

Figure 3. Differentially expressed proteins in WT vs myo$^{-/-}$ mice related to intermediary metabolism. For the complete list of altered proteins, refer to online Table IV. Data are mean±SD (n=12, *P<0.005, **P<0.0005, ***P<0.00005 vs WT). DH indicates dehydrogenase; ETF, electron transferring flavoprotein; GAP, glyceraldehyde 3-phosphate; HI/HII, hydrogenase isoform I/II; IV, isovaleryl; SC; short chain; TFP, trifunctional protein.

mice (6.7±2.3%ID versus 0.8±0.5%ID in WT, n=5; P<0.001).

Analysis of Blood Serum Substrates

Both ^{13}C NMR and PET data indicate a shift to increased glucose and reduced fatty acid utilization in transgenic hearts. To clarify whether these alterations may have been caused by differences in serum substrate concentrations, we determined the amounts of glucose, lactate, and various FAs (16:0, 16:1, 18:0, 18:1, 20:0, 20:1, 20:2, 20:3, and 20:4) in WT and myo$^{-/-}$ mice (n=6). However, there were no significant differences between the 2 groups concerning all parameters analyzed (data are given in online Table III).

Proteome Analysis

To investigate whether the observed alterations in cardiac metabolism are related to changes in myocardial protein expression, proteome patterns of WT and myo$^{-/-}$ mice were analyzed by 2D-PAGE (see Figure II in the online data supplement for representative gels). Aside from Mb, 21 protein species were found to be differentially expressed when comparing myo$^{-/-}$ with WT samples (online Table IV). Noticeably, more than half of the altered proteins are involved in intermediary metabolism (Figure 3), and 9 of these are part of the mammalian mitochondrial β-oxidation pathway,[14] which is illustrated in the schematic drawing of Figure 4. The first step of the β-oxidation spiral is catalyzed by acyl-CoA dehydrogenases (DHs), which lead to the oxidation of acyl-CoA to enoyl-CoA by FAD. Two members of this enzyme family, short-chain and isovaleryl acyl-CoA DH, were reduced in expression by ≈ 50%. The next steps of β-oxidation are mediated by enoyl-CoA hydratases: two forms of the short-chain FA selective soluble enzyme were decreased in expression by 58% and 33% in myo$^{-/-}$ hearts.

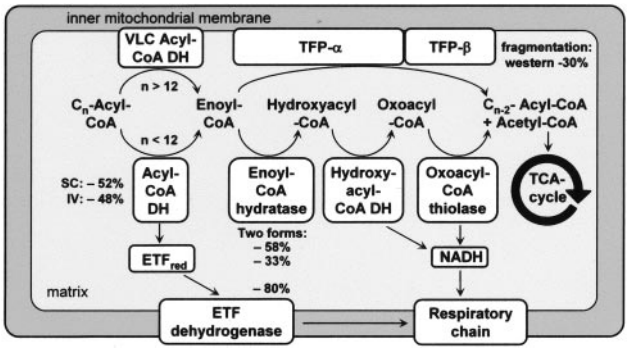

Figure 4. Schematic drawing of key steps of mitochondrial β-oxidation incorporating the observed alterations in protein expression of myo$^{-/-}$ hearts (changes in percent relative to WT hearts). DH indicates dehydrogenase; ETF, electron transferring flavoprotein; IV, isovaleryl; SC; short chain; TFP, trifunctional protein; VLC, very long chain.

The membrane-bound enoyl-CoA hydratase (selective for long-chain FAs) is part of the α-subunit of mitochondrial trifunctional protein (TFP), which combines 3 long-chain (LC) FA selective enzymatic activities: LC enoyl-CoA hydratase and LC 3-hydroxyacyl-CoA DH, both located on the α-subunit, as well as LC 3-ketoacyl-CoA-thiolase, located on the β-subunit.[15] Whereas 2D-PAGE analysis did not reveal a difference in expression of the intact α- and β-subunits of TFP between the groups, 4 cleavage fragments of α-TFP were prominently found on gels of Mb mutant hearts (Figure 3). Similarly, fragments of the β-subunit were clearly visible in myo$^{-/-}$ samples. Western blot analysis using a polyclonal antibody raised against the β-subunit of TFP[16] revealed a downregulation of the intact subunit by 30% (n=9 per group, P<0.05). Furthermore, we found the membrane-bound enzyme electron-transferring flavoprotein DH (ETF DH), which feeds the reduction equivalents into the respiratory chain (Figure 4) to be downregulated by 80% in the knockout (Figure 3). On the other hand, the glycolytic enzyme glyceraldehyde 3-phosphate DH was significantly upregulated (+420%) in myo$^{-/-}$ hearts (Figure 3). For a more detailed description of the proteome data including the other differentially expressed proteins refer to the online data supplement.

Because GLUT4 is the major transport system for uptake of glucose into cardiomyocytes,[17] we further verified whether the enhanced glucose utilization in Mb-deficient hearts is associated with alterations in overall cardiac GLUT4 expression and/or translocation of this transporter from the cytosol to the plasma membrane. Western blot analysis revealed GLUT4 expression to be significantly increased in both the cytosolic and the membranous fraction of myo$^{-/-}$ as compared with WT heart extracts (Figure 5). However, it is noteworthy that the relative raise of the transporter in the plasma membrane (60%) is more pronounced than in the cytosol (20%), which reflects in addition to an increased expression an enhanced translocation of GLUT4 into the membrane.

Gene Expression

We further analyzed whether the altered expression of enzymes of FA oxidation relates to a gene regulatory switch.

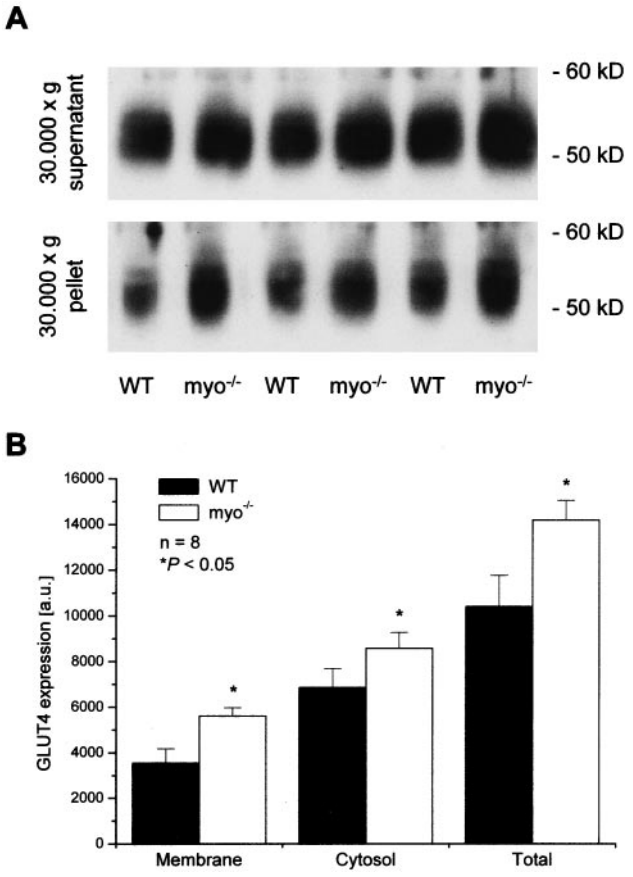

Figure 5. GLUT4 expression in membranous and cytosolic fractions of WT and myo$^{-/-}$ hearts. A, Representative Western blots. B, Densitometric quantification. Data are mean±SD (n=8, *P<0.05 vs WT)

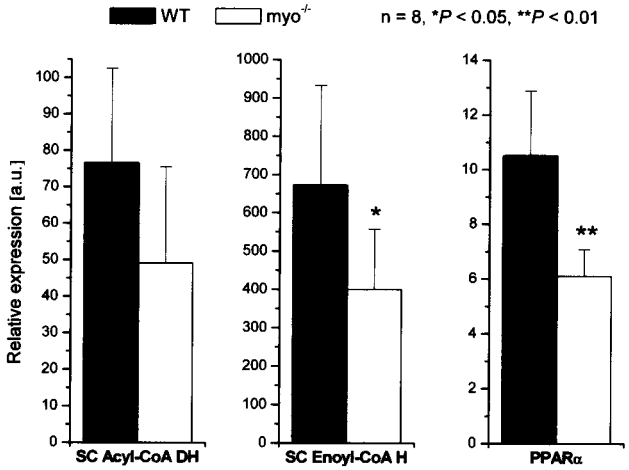

Figure 6. mRNA levels of selected proteins in hearts of WT and myo$^{-/-}$ mice. Data are mean±SD (n=8, *P<0.05, **P<0.01 vs WT). DH indicates dehydrogenase; H, hydrogenase, PPAR, peroxisome proliferator activated receptor; SC; short chain.

For this purpose, we measured mRNA levels of a subset of proteins that were downregulated in Mb-deficient hearts and, additionally, the expression of the nuclear receptor PPARα (peroxisome proliferator activated receptor α), which has been shown to be a key factor in regulation of several genes involved in β-oxidation of fatty acids.[18] Transcripts of short-chain acyl-CoA DH and enoyl-CoA hydratase were found to be reduced in myo$^{-/-}$ hearts by ≈40% to 50% (Figure 6), which fits well to the alterations observed at the translated protein level (Figure 3). Furthermore, expression of PPARα was decreased by a similar extent (≈40%) in the transgenic group (Figure 6, right; WT: 10.5±2.4 AU, myo$^{-/-}$: 6.1±1.0 AU, n=8; P<0.01).

Discussion

The results of the present study show that lack of Mb causes a shift from free FA to glucose oxidation in cardiac energy production. Enhanced glucose uptake in myo$^{-/-}$ hearts was noninvasively visualized by FDG-PET in vivo and the substrate switch was confirmed by ^{13}C NMR isotopomer studies of isolated hearts. Protein and gene expression analysis demonstrated that the most abundant glucose transporter in the heart, GLUT4, is upregulated whereas important enzymes of mitochondrial β-oxidation and the key regulator of genes involved in FA metabolism, PPARα, are downregulated in Mb-deficient hearts. Based on these data and the finding that cardiac structure and function remained fully unchanged in myo$^{-/-}$ hearts, it appears that Mb is a critical determinant of cardiac substrate selection.

Quantitative evaluation of the individual substrate fluxes in WT hearts revealed a utilization of FAs more than glucose in the order of 3:1, which is close to the normal situation in humans.[3] In contrast, myo$^{-/-}$ hearts used approximately equal amounts of FAs and glucose. This shift in substrate utilization in myo$^{-/-}$ hearts resembles the known differences in metabolism of red and white muscle. Early investigations on the enzyme pattern of white (fast) and red (slow) muscles showed that white muscle fibers contain high amounts of glycolytic enzymes, whereas red muscles predominantly express enzymes of the β-oxidation pathway.[1] The analogy to skeletal muscle is further supported by the observed differences in expression level of α-(B)-crystallin in myo$^{-/-}$ and WT hearts (online Table IV), which is also similar to that found between white and red muscle.[19]

The correlation of myocardial Mb content with the capacity of β-oxidation has been described in previous studies under both physiological and pathophysiological conditions. In a recent study of the heterogeneity of cardiac flow and metabolism, we showed that certain areas in the well-perfused dog heart that normally receive <50% of mean myocardial blood flow exhibited reduced Mb levels accompanied by decreased expression of enzymes of the β-oxidation pathway and enhanced expression of glycolytic enzymes.[10] Studies in canine and bovine models of dilated cardiomyopathy also demonstrated a reduced expression of Mb and concomitant upregulation of glycolytic and/or downregulation of β-oxidation enzymes.[20,21] Together with the results of the present work, these data suggest a causal relationship between myocytic Mb content and β-oxidation of fatty acids. As to the molecular mechanisms involved,

several possibilities must be considered by which Mb might directly or indirectly affect muscle substrate selection.

Mb is generally thought not only to provide the O_2 needed for aerobic muscle metabolism and to augment the flow of O_2 to the mitochondria but also to buffer intracellular O_2 concentrations in response to mitochondrial demand.[22] A possible mismatch between O_2 requirement and O_2 supply because of the lack of Mb could be overcome by a shift from FA oxidation to O_2-sparing glucose utilization. It is well known that the complete oxidation of FAs consumes more O_2 per mole energy-rich phosphate than the complete oxidation of glucose. On basis of the respective phosphate-to-oxygen ratios (P:O) myocardial O_2 consumption (MVO_2) can be assumed to increase by ≈10% when FAs are exclusively utilized as compared with glucose.[23] This value, however, may be an underestimation, because it has been recently demonstrated in the in vivo unloaded myocardium that FA usage requires 48% more O_2 when compared with glucose.[24] MVO_2 measurements in the present study have shown an oxygen saving of 7.5% (at a shift of glucose/FA utilization from ≈1:3 to an equal ratio), which supports the notion of the latter study that the benefit of using glucose may be considerably higher as calculated on basis of the P:O ratios. Thus, a shift toward glucose oxidation will improve the O_2 balance in the Mb-deficient heart and may be considered as a molecular adaptation mechanism in the myo$^{-/-}$ heart.

Besides its function in O_2 storage and transport, Mb has also been suggested to support ATP generation by cardiac cells under conditions of fully oxygenated Mb: a phenomenon referred to as Mb-mediated oxidative phosphorylation.[25] As an underlying mechanism, a preferred uptake of Mb-bound O_2 by mitochondria and/or the acceptance of electrons by sarcoplasmic Mb with concomitant reduction of heme iron-ligated O_2 to H_2O were suggested. However, because an enhanced oxidative phosphorylation would support aerobic oxidation of both glucose and FAs, it is rather unlikely that an impaired Mb-mediated oxidative phosphorylation causes the metabolic shift in hearts lacking Mb.

In addition to its function as respiratory pigment, Mb of bovine, chicken, and rat muscle was shown to bind FAs.[26–28] Therefore, Mb has been suggested to function as transport protein for FAs in the cytosol working in concert with the well-known fatty acid binding protein, which is generally assumed to be the major player.[29] Interestingly, FA binding of Mb depends on its oxygenation in that conformational changes induced by O_2 binding favor the interaction of Mb with FAs.[28] Although the functional relevance of FA binding to Mb remains to be explored, the simultaneous delivery of O_2 and FAs to mitochondria would clearly be advantageous for aerobically working muscle. According to this hypothesis, lack of Mb as putative FA carrier would supply less substrate to the mitochondria, thereby triggering the downregulation of β-oxidation to total energy production of myo$^{-/-}$ hearts.[30]

Because we have previously shown that Mb substantially contributes to NO breakdown in the heart,[31] it is conceivable that increased levels of NO as a result of diminished NO degradation may affect cardiac metabolism in Mb-deficient hearts. Indeed, it has been demonstrated that NO is involved in stimulation of glucose uptake and metabolism (eg, via GLUT4 translocation) particularly in skeletal[32] but also in heart muscle.[33,34] Furthermore, it has also been described that endogenous NO reduces O_2 use in excitation-contraction coupling and attenuates cardiac contractility without changing contractile efficiency.[35] This could further contribute to improved O_2 balance in the Mb-deficient heart.

It is becoming increasingly evident that protein-protein interactions within the living cell are important in various cellular signal transduction pathways, and that in vivo, many proteins do not work by themselves but, in most cases, by forming a complex or interacting with other proteins, DNA, RNA, or ligands (interactome).[36] However, little is known about the interactome of Mb, albeit dynamic docking and electron transfer between Mb and cytochrome b5 have lately been discovered.[37] Furthermore, there is recent evidence that the ferric form of neuroglobin, which is homologous to Mb, acts as a heterotrimeric Gα protein guanine nucleotide dissociation inhibitor thereby shutting off signaling pathways linked to Gα effectors and favoring G$\alpha\gamma$ effector pathways leading to protection against neuronal death.[38] Because Mb is present in the cytosol in high concentrations (up to 0.5 mmol/L) it is quite conceivable that multiple interactions with other cellular proteins exist, which—when lacking—may cause metabolic rearrangements.

Taken together the combined effect of Mb's different biological functions is likely to trigger the changes in intermediary metabolism when Mb is lacking. Decreased mitochondrial O_2 availability and increased amounts of bioactive NO may act as complementary players in this process: because lack of Mb results in an enhanced vulnerability to mild or short periods of hypoxic/ischemic conditions,[39] it is conceivable that even the unstressed Mb-deficient heart is characterized by a "microhypoxic" environment promoting the expression of hypoxia-responsive genes,[8] which have been described to mediate inhibition of expression of the nuclear receptor PPARα.[40] The NO-induced stimulation of expression and translocation of GLUT4[34] together with the recently proposed regulatory "crosstalk" between PPARα signaling and GLUT4 gene expression[41] could provide the molecular framework of the observed substrate switch to an increased glucose utilization. Note that, conversely, transgenic mice with cardiac-specific overexpression of PPARα exhibit increased fatty acid uptake and oxidation as well as reciprocal inhibition of glucose uptake and metabolism.[42]

Similar shifts in cardiac substrate selection as described in this study for the myo$^{-/-}$ mouse have been frequently reported to occur during hypertrophy and several other cardiac diseases (see reviews[43,44]). It has been postulated that this rearrangement of cardiac energy production contributes to the compensated state during progression to heart failure.[43,44] Metabolic remodeling has been as yet seen as part of the reactivation of the fetal gene expression program typically observed during development of left ventricular hypertrophy. However, there is no evidence for an upregulation of atrial natriuretic peptide and skeletal muscle actin or other markers of the fetal gene expression program in myo$^{-/-}$ hearts.[45] Furthermore, it should be noted that in this and previous studies we and others found no indication for an impaired cardiac function in Mb-deficient mice under normal condi-

tions.[6,7] Therefore, the Mb knockout mouse clearly illustrates that metabolic remodeling represents an important compensatory mechanism that can be activated independent of the fetal gene expression program. Thus, this model can be used in future studies to determine the potentially protective role of increased glucose utilization in certain pathological states like ischemia and/or diabetes without interference of mechanisms governed by the reactivation of the fetal gene expression program.

In summary, our data show that lack of Mb leads to an enhanced glucose and a decreased FA utilization in the mouse heart. Because equimolar production of ATP from glucose consumes less O_2 than from FAs, this metabolic switch may be viewed as an additional adaptive mechanism in myo$^{-/-}$ hearts. The changes in substrate selection of Mb-deficient hearts resemble the well-known differences in metabolic pattern of red and white muscle. Our data suggest that an altered Mb level by itself is one crucial factor that determines the relative utilization of FAs versus glucose, thus placing Mb in a central stage within the regulatory network that controls cardiac energy production.

Acknowledgments

This study was supported by the Biologisch-Medizinisches Forschungszentrum of the Heinrich-Heine-Universität Düsseldorf, the Sonderforschungsbereich 612 "Molekulare Analyse kardiovaskulärer Funktionen and Funktionsstörungen", Teilprojekt Z2, and in part by the Interdisziplinäres Zentrum für Klinische Forschung (IZKF), Münster, Germany (grant ZPG 4 to M.S.). We thank D. Haubs, S. Küsters, and C. Kirberich for excellent technical assistance, and R. Hoffmann and S. Lauter for their expert help in protein identification by ESI-MS/MS. We thank A. Strauss from the Department of Pediatrics at Vanderbilt University, Nashville, Tenn, for providing us with anti-TFP antibody.

References

1. Bass A, Brdiczka D, Eyer P, Hofer S, Pette D. Metabolic differentiation of distinct muscle types at the level of enzymatic organization. *Eur J Biochem*. 1969;10:198–206.
2. Hoppeler H. Skeletal muscle substrate metabolism. *Int J Obes Relat Metab Disord.* 1999;23:S7–S10.
3. Lopaschuk GD, Belke DD, Gamble J, Itoi T, Schonekess BO. Regulation of fatty acid oxidation in the mammalian heart in health and disease. *Biochim Biophys Acta*. 1994;1213:263–276.
4. Sambandam N, Lopaschuk GD, Brownsey RW, Allard MF. Energy metabolism in the hypertrophied heart. *Heart Fail Rev*. 2002;7:161–173.
5. O'Brien PJ, Gwathmey JK. Myocardial Ca^{2+}- and ATP-cycling imbalances in end-stage dilated and ischemic cardiomyopathies. *Cardiovasc Res*. 1995;30:394–404.
6. Garry DJ, Ordway GA, Lorenz JN, Radford NB, Chin ER, Grange RW, Bassel-Duby R, Williams RS. Mice without myoglobin. *Nature*. 1998; 395:905–908.
7. Gödecke A, Flögel U, Zanger K, Ding Z, Hirchenhain J, Decking UK, Schrader J. Disruption of myoglobin in mice induces multiple compensatory mechanisms. *Proc Natl Acad Sci U S A*. 1999;96:10495–10500.
8. Meeson AP, Radford N, Shelton JM, Mammen PP, DiMaio JM, Hutcheson K, Kong Y, Elterman J, Williams RS, Garry DJ. Adaptive mechanisms that preserve cardiac function in mice without myoglobin. *Circ Res*. 2001;88:713–720.
9. Flögel U, Decking UK, Gödecke A, Schrader J. Contribution of NO to ischemia-reperfusion injury in the saline-perfused heart: a study in endothelial NO synthase knockout mice. *J Mol Cell Cardiol*. 1999;31: 827–836.
10. Laussmann T, Janosi RA, Fingas CD, Schlieper GR, Schlack W, Schrader J, Decking UK. Myocardial proteome analysis reveals reduced NOS inhibition and enhanced glycolytic capacity in areas of low local blood flow. *FASEB J*. 2002;16:628–630.
11. Nürnberg B. Pertussis toxin as a pharmacological tool. In: Aktories K, Just I, eds. *Handbook of Experimental Pharmacology, vol 145: Bacterial Protein Toxins*. Berlin, Heidelberg: Springer Verlag; 2000:187–206.
12. Tusher VG, Tibshirani R, Chu G. Significance analysis of microarrays applied to the ionizing radiation response. *Proc Natl Acad Sci U S A*. 2001;98:5116–5121.
13. Malloy CR, Thompson JR, Jeffrey FM, Sherry AD. Contribution of exogenous substrates to acetyl coenzyme A: measurement by ^{13}C NMR under non-steady-state conditions. *Biochemistry*. 1990;29:6756–6761.
14. Eaton S, Bartlett K, Pourfarzam M. Mammalian mitochondrial β-oxidation. *Biochem J*. 1996;320:345–357.
15. Uchida Y, Izai K, Orii T, Hashimoto T. Novel fatty acid β-oxidation enzymes in rat liver mitochondria. II. Purification and properties of enoyl-coenzyme A (CoA) hydratase/3-hydroxyacyl-CoA dehydrogenase/3-ketoacyl-CoA thiolase trifunctional protein. *J Biol Chem*. 1992;267: 1034–1041.
16. Ibdah JA, Paul H, Zhao Y, Binford S, Salleng K, Cline M, Matern D, Bennett MJ, Rinaldo P, Strauss AW. Lack of mitochondrial trifunctional protein in mice causes neonatal hypoglycemia and sudden death. *J Clin Invest*. 2001;107:1403–1409.
17. Abel ED. Glucose transport in the heart. *Front Biosci*. 2004;9:201–215.
18. Barger PM, Kelly DP. PPAR signaling in the control of cardiac energy metabolism. *Trends Cardiovasc Med*. 2000;10:238–245.
19. Neufer PD, Benjamin IJ. Differential expression of B-crystallin and Hsp27 in skeletal muscle during continuous contractile activity. Relationship to myogenic regulatory factors. *J Biol Chem*. 1996;271: 24089–24095.
20. O'Brien PJ, O'Grady M, McCutcheon LJ, Shen H, Nowack L, Horne RD, Mirsalimi SM, Julian RJ, Grima EA, Moe GW. Myocardial myoglobin deficiency in various animal models of congestive heart failure. *J Mol Cell Cardiol*. 1992;24:721–730.
21. Weil J, Eschenhagen T, Magnussen O, Mittmann C, Orthey E, Scholz H, Schafer H, Scholtysik G. Reduction of myocardial myoglobin in bovine dilated cardiomyopathy. *J Mol Cell Cardiol*. 1997;29:743–751.
22. Wittenberg JB, Wittenberg BA. Myoglobin function reassessed. *J Exp Biol*. 2003;206:2011–2020.
23. Suga H. Ventricular energetics. *Physiol Rev*. 1990;70:247–277.
24. Korvald C, Elvenes OP, Myrmel T. Myocardial substrate metabolism influences left ventricular energetics in vivo. *Am J Physiol Heart Circ Physiol*. 2000;278:H1345–H1351.
25. Wittenberg BA, Wittenberg JB. Myoglobin-mediated oxygen delivery to mitochondria of isolated cardiac myocytes. *Proc Natl Acad Sci U S A*. 1987;84:7503–7507.
26. Gloster J, Harris P. Fatty acid binding to cytoplasmic proteins of myocardium and red and white skeletal muscle in the rat: a possible new role for myoglobin. *Biochem Biophys Res Commun*. 1977;74:506–513.
27. Moore KK, Cameron PJ, Ekeren PA, Smith SB. Fatty acid-binding protein in bovine longissimus dorsi muscle. *Comp Biochem Physiol B*. 1993;104:259–266.
28. Götz FM, Hertel M, Groschel-Stewart U. Fatty acid binding of myoglobin depends on its oxygenation. *Biol Chem Hoppe Seyler*. 1994;375:387–392.
29. van der Vusse GJ, van Bilsen M, Glatz JF. Cardiac fatty acid uptake and transport in health and disease. *Cardiovasc Res*. 2000;45:279–293.
30. Augustus A, Yagyu H, Haemmerle G, Bensadoun A, Vikramadithyan RK, Park SY, Kim JK, Zechner R, Goldberg IJ. Cardiac-specific knock-out of lipoprotein lipase alters plasma lipoprotein triglyceride metabolism and cardiac gene expression. *J Biol Chem*. 2004;279: 25050–25057.
31. Flögel U, Merx MW, Gödecke A, Decking UK, Schrader J. Myoglobin: A scavenger of bioactive NO. *Proc Natl Acad Sci U S A*. 2001;98: 735–740.
32. Young ME, Radda GK, Leighton B. Nitric oxide stimulates glucose transport and metabolism in rat skeletal muscle in vitro. *Biochem J*. 1997;322:223–228.
33. McFalls EO, Hou M, Bache RJ, Best A, Marx D, Sikora J, Ward HB. Activation of p38 MAPK and increased glucose transport in chronic hibernating swine myocardium. *Am J Physiol Heart Circ Physiol*. 2004; 287:H1328–H1334.
34. Li J, Hu X, Selvakumar P, Russell RR III, Cushman SW, Holman GD, Young LH. Role of the nitric oxide pathway in AMPK-mediated glucose uptake and GLUT4 translocation in heart muscle. *Am J Physiol Endocrinol Metab*. 2004;287:E834–E841.
35. Suto N, Mikuniya A, Okubo T, Hanada H, Shinozaki N, Okumura K. Nitric oxide modulates cardiac contractility and oxygen consumption without changing contractile efficiency. *Am J Physiol*. 1998;275:H41–H49.

36. Gerstein M, Lan N, Jansen R. Proteomics: integrating interactomes. *Science*. 2002;295:284–287.
37. Liang ZX, Nocek JM, Huang K, Hayes RT, Kurnikov IV, Beratan DN, Hoffman BM. Dynamic docking and electron transfer between Zn-myoglobin and cytochrome b(5). *J Am Chem Soc*. 2002;124:6849–6859.
38. Wakasugi K, Nakano T, Morishima I. Oxidized human neuroglobin acts as a heterotrimeric Gα protein guanine nucleotide dissociation inhibitor. *J Biol Chem*. 2003;278:36505–36512.
39. Merx MW, Flögel U, Stumpe T, Gödecke A, Decking UK, Schrader J. Myoglobin facilitates oxygen diffusion. *FASEB J*. 2001;15:1077–1079
40. Narravula S, Colgan SP. Hypoxia-inducible factor 1-mediated inhibition of peroxisome proliferator-activated receptor α expression during hypoxia. *J Immunol*. 2001;166:7543–7548.
41. Finck BN, Bernal-Mizrachi C, Ho Han D, Coleman T, Sambandam N, LaRiviere LL, Holloszy JO, Semenkovich F, Kelly DP. A potential link between muscle peroxisome proliferator-activated receptor-α signaling and obesity-related diabetes. *Cell Metab*. 2005;1:133–144.
42. Finck BN, Lehman JJ, Leone TC, Welch MJ, Bennett MJ, Kovacs A, Han X, Gross RW, Kozak R, Lopaschuk GD, Kelly DP. The cardiac phenotype induced by PPARα overexpression mimics that caused by diabetes mellitus. *J Clin Invest*. 2002;109:121–130.
43. van Bilsen M. "Energenetics" of heart failure. *Ann N Y Acad Sci*. 2004; 1015:238–249.
44. Taegtmeyer H, Golfman L, Sharma S, Razeghi P, van Arsdall M. Linking gene expression to function: metabolic flexibility in the normal and diseased heart. *Ann N Y Acad Sci*. 2004;1015:202–213.
45. Gödecke A, Molojavyi A, Heger J, Flögel U, Ding Z, Jacoby C, Schrader J. Myoglobin protects the heart from inducible nitric-oxide synthase (iNOS)-mediated nitrosative stress. *J Biol Chem*. 2003;278:21761–21766.

Circulation Research
JOURNAL OF THE AMERICAN HEART ASSOCIATION

Lack of Myoglobin Causes a Switch in Cardiac Substrate Selection

Ulrich Flögel, Tim Laussmann, Axel Gödecke, Nadine Abanador, Michael Schäfers, Christian Dominik Fingas, Sabine Metzger, Bodo Levkau, Christoph Jacoby and Jürgen Schrader

Circ Res. 2005;96:e68-e75; originally published online April 7, 2005;
doi: 10.1161/01.RES.0000165481.36288.d2
Circulation Research is published by the American Heart Association, 7272 Greenville Avenue, Dallas, TX 75231

Print ISSN: 0009-7330. Online ISSN: 1524-4571

ONLINE DATA SUPPLEMENT

MATERIALS AND METHODS

Heart perfusion

General setup: Preparation of hearts and retrograde, non-recirculating perfusion at constant pressure of 100 mmHg with modified Krebs-Henseleit buffer – gassed at 95% O_2/5% CO_2 (carbogen), resulting in a pH of 7.4 – was performed essentially as described.[1] Perfusion pressure, coronary flow, and left ventricular developed pressure were measured continously. Signals were recorded with a sampling rate of 100 Hz utilizing a PC with dedicated software (ADInstruments, USA). Hearts were kept at 37 °C using a water-temperated glass jacket. After hearts had stabilized, cardiac pacing (500 bpm) was initiated and continued throughout. 30 minutes after onset of cardiac pacing, the coronary perfusion rate was fixed to the steady flow established and was maintained constant. Hearts were subsequently supplied with buffer which contained 5 mM glucose, 0.5 mM palmitate (bound to 3% albumin), and 50 µU insulin and was gassed at 95%O_2/5%CO_2 *via* a home-made bulb oxygenator.

Metabolic analysis: After hemodynamic and contractile parameters maintained constant under these conditions, hearts were finally switched to buffer containing 5 mM [1,6-$^{13}C_2$]glucose, 0.5 mM [U-$^{13}C_{16}$]palmitate (both from Cambridge Isotope Laboratories (Andover, USA), the latter bound to 3% essentially fatty acid free albumin), and 50 µU insulin. After 25 min of perfusion hearts were freeze-clamped, extracted with perchloric acid (PCA), neutralized, lyophilized, and stored at -20° C.

Measurement of myocardial oxygen consumption: Arterial and venous PO_2 were measured simultaneously with implantable oxygen micro-sensors based on 140 µm optical silica fiber

(Presens; Regensburg, Germany). For determination of arterial PO_2 one sensor was introduced *via* a branch connection into the perfusion line and positioned right in front of the aorta. Coronary venous PO_2 was measured by a second sensor which was advanced *via* the pulmonary artery into the right ventricle. Sensors were connected to a four-channel oxygen meter (OXY-4 micro) and signals were recorded continously with a sampling rate of 0.3 Hz by using a notebook with dedicated software (Presens, Regensburg, Germany). Oxygen consumption was calculated according to Fick's principle as the product of the arterio-venous O_2 content difference and coronary flow. Data were normalized for heart weights.

Magnetic resonance measurements

Data were recorded on a Bruker DRX 9.4 Tesla WB NMR spectrometer operating at frequencies of 400.1 MHz for ^{1}H measurements and 100.6 MHz for ^{13}C measurements.

Spectroscopy: Lyophilized PCA extracts were redissolved in 0.5 ml D_2O. Spectra were recorded from a 5-mm $^{1}H/^{13}C$ dual probe. ^{1}H NMR spectra were acquired with a flip angle of 90º, repetition time 15 s, low power water presaturation, 512 scans, spectral width 5580 Hz, data size 16 K, zero filling to 32 K. Chemical shifts were referenced to (trimethylsilyl)-propionic-2,2,3,3d_4-acid (TSP) at 0 ppm. For ^{13}C NMR spectra 20 K scans were accumulated with a flip angle of 30º, repetition time 1.7 s, composite pulse decoupling with Waltz16, spectral width 25062 Hz, data size 32 K, zero filling to 64 K, exponential weighting resulting in a 1 Hz line broadening. Chemical shifts were referenced to C3 of lactate at 21.3 ppm.

Imaging: Magnetic resonance imaging (MRI) was performed using a microimaging unit (Mini 0.5, Bruker) equipped with an actively shielded 57-mm gradient set (capable of

200 mT/m maximum gradient strength and 110 µs rise time at 100% gradient switching) and a 38-mm birdcage resonator. Mice were slightly anaesthetized with isoflurane (1.5%) and kept at 37° C. High resolution images of mice hearts were acquired using an electrocardiogram- and respiration-triggered fast gradient echo cine sequence with a flip angle < 30°, echo time < 2 ms, and a repetition rate of about 4 ms. The resulting in-plane resolution was 117·117 μm^2 (field of view 30·30 mm^2, 256·256 matrix, 1 mm slice thickness). The total acquisition time per slice for one cine sequence was about 2 min. Six to eight contiguous ventricular short axis slices were acquired to cover the entire heart.

Isotopomer analysis of carbon flow into the TCA cycle: The pool size of various metabolites has been determined from fully relaxed ^{1}H NMR spectra of extracts from hearts perfused with unlabelled substrates and are given in table 1 of this section. Quantitative evaluation of the spectra was done by using the mixed lorentzian/gaussian deconvolution availabe under X-WinNMR 2.6 (Bruker). The implemented automatic integration routine resulted in relative peak areas. TSP was used to standardize the concentration and integrated values were related to the protein content (Lowry) and converted to concentrations on the basis of a cytosolic water space of 4.3 µl/mg protein.[1] ^{13}C NMR spectra were corrected for natural abundant ^{13}C and were quantified as previously described.[2] The relative contributions of palmitate ($F_{Palmitate}$), glucose ($F_{Glucose}$), and endogenous sources ($F_{Endogenous}$) to the total acetyl-CoA pool entering the TCA cycle were determined from isotopomer analysis of glutamate carbons C3 and C4 only,[3] since S/N ratio of mouse heart ^{13}C NMR spectra was not sufficient to examine accurately glutamate carbon C2 in each case. Fluxes were calculated from the doublet due to J_{34} coupling (C4D34), the quartet or doublet of doublets (C4Q) due to J_{345} coupling (*cf.*

fig. 1), and the ratio of the total resonance areas of glutamate carbons C4 and C3 (C4/C3), *cf.* reference 3 for a detailed derivation of the following equations:

(1) $F_{Glucose} = (C4D34)/(C4/C3)$

(2) $F_{Palmitate} = (C4Q)/(C4/C3)$

(3) $F_{Endogenous} = 1 - F_{Glucose} - F_{Palmitate}$

Proteome analysis

Sample preparation and 2D-PAGE were essentially performed as previously reported.[4] In brief, following thoracotomy hearts were perfused *in situ* by phosphate-buffered saline, excised, weighted, and immediately lysed. After tissue homogenization and centrifugation at 14000 rpm (10 °C, 10 min) samples were divided into 50 µl aliquots and stored at -80 °C. For isoelectric focussing (IEF) immobilized pH gradients (IPGs) and the IPGphor system (Amersham Pharmacia Biotech) were used. Rehydration of IPG strips (24 cm, pH 3-10 linear gradient; containing 150 µg protein for analytical gels and up to 2 mg protein for preparative gels) and IEF were carried out as described.[2] SDS-PAGE was performed on a ETTAN-DALT II vertical electrophoresis unit (Amersham Pharmacia Biotech). Equilibrated IPG strips were placed on top of the gel (size of $0.1 \cdot 25.5 \cdot 20$ cm^3) and fixed in place by agarose sealing solution.[5] Twelve gels were run simultaneously (settings: 30 min, 30 W; 4.5 h, 180 W) and either silver-stained[6] or stained by coomassie blue R250.

Image analysis: The gels were digitized at 300 dpi, 8 bit gray scale, blue channel using a UMAX PowerLook III scanner calibrated by a photographic step tablet (Kodak). Images were

evaluated by the Image Master 2D Elite 3.10 software (Amersham Pharmacia Biotech). Background substraction was performed by the "mode of non spot" option (setting: 45 pixel). All spot volumes, *i.e.* spot area multiplied by the mean gray value, were divided by the sum of the volume of all spots detected on the gel. Faint spots (spot volume < 0.02 %) and doubtful spots (irreproducible, clustered or smeared) were excluded from the statistical analysis. A reference gel containing 583 valid spots was created from gels of 5 WT and 5 myo$^{-/-}$ samples and served as an index to the spots on individual gels.

RESULTS

Metabolite pool sizes

No differences were observed in pool sizes of metabolites (table 1) and fractional enrichments (data not shown) of alanine, glutamate, and lactate between WT and myo$^{-/-}$ hearts.

In vivo MRI analysis

Prior to PET analysis all mice were initially characterized by MRI which showed similar values for diastolic and systolic volumes as well as cardiac output in both groups (table 2).

Analysis of blood serum substrates

Both ^{13}C NMR and PET data indicate a shift to increased glucose and reduced fatty acid utilization transgenic hearts. To clarify whether these alterations may have been caused by differences in serum substrate concentrations, we determined the amounts of glucose, lactate, and various FAs (16:0, 16:1, 18:0, 18:1, 20:0, 20:1, 20:2, 20:3, 20:4) in WT and myo$^{-/-}$ mice (n=6). However, there were no significant differences between the two groups concerning all parameters analyzed (table 3).

Proteome analysis

Approximately 460 different protein species were recorded on each gel (fig. 2), with similar numbers of spots in both groups (466±18 in WT and 455±26, in myo$^{-/-}$, n=12 each). Besides Mb, 21 protein species were found to be differentially expressed when comparing myo$^{-/-}$ with WT samples (table 4): Eleven protein species showed decreased and 10 increased expression in myo$^{-/-}$ hearts. Noticeably, more than half of the proteins that were differentially expressed are involved in intermediary metabolism (table 4). Classification of the other altered proteins is less homogenous: five of them can be assigned to the group of stress proteins, whereas the remaining 5 proteins cannot be summed up under a common category. Ten of the 21 altered protein species are involved in FA metabolism (table 4). Nine of these are part of the mammalian mitochondrial β-oxidation pathway which are discussed in detail in the normal manuscript.

Further differentially expressed proteins (table 4 of this section lists all altered proteins determined by 2D-PAGE): Two chaperon related proteins were altered in expression: mitochondrial stress-70 protein (+160% in myo$^{-/-}$ vs. WT) and the α-subunit of (B)-crystallin (–38%). Furthermore, at unchanged expression level the antioxidant protein 2 (AOP2) showed a shift in the isoelectric point from pH 6.42 in WT to pH 6.05 in myo$^{-/-}$ mice. Sequence analysis of the proteins cDNA revealed alanine at position 123 to be replaced by asparagic acid in myo$^{-/-}$ hearts which can easily explain the shift in the isoelectric point. The same sequence variant of AOP2 has also been described elsewhere.[7] Mitochondrial manganese superoxide dismutase was found to be reduced by 69 % in myo$^{-/-}$ mice. Moreover, a prominent protein of the outer mitochondrial membrane, the voltage-dependent anion channel 1 was found to be decreased by 60% in Mb deficient hearts. Fumarate hydratase

which catalyses the dehydration of malate to fumarate exhibited less expression in myo$^{-/-}$ hearts, while other enzymes of the TCA cycle were not found to be differentially expressed. Additionally, we found that apolipoprotein A1 which is involved in serum lipid transport is reduced by 73% in hearts of Mb-deficient mice.

REFERENCES

1. Flögel U, Decking UK, Gödecke A, Schrader J. Contribution of NO to ischemia-reperfusion injury in the saline-perfused heart: a study in endothelial NO synthase knockout mice. *J Mol Cell Cardiol*. 1999;31:827-836.
2. Flögel U, Willker W, Leibfritz D. Determination of de novo synthesized amino acids in cellular proteins revisited by ^{13}C NMR spectroscopy. *NMR Biomed*. 1997;10:50-58.
3. Malloy CR, Thompson JR, Jeffrey FM, Sherry AD. Contribution of exogenous substrates to acetyl coenzyme A: measurement by ^{13}C NMR under non-steady-state conditions. *Biochemistry*. 1990;29:6756-6761.
4. Laussmann T, Janosi RA, Fingas CD, Schlieper GR, Schlack W, Schrader J, Decking UK. Myocardial proteome analysis reveals reduced NOS inhibition and enhanced glycolytic capacity in areas of low local blood flow. *FASEB J*. 2002;16:628-630.
5. Li Y, Huang TT, Carlson EJ, Melov S, Ursell PC, Olson JL, Noble LJ, Yoshimura MP, Berger C, Chan PH, . Dilated cardiomyopathy and neonatal lethality in mutant mice lacking manganese superoxide dismutase. *Nat Genet*. 1995;11:376-381.
6. Blum H, Gross HJ, Beier H. Improved silver staining of plant proteins, RNA and DNA in polyacrylamide gels. *Electrophoresis*. 1987;8:83-89.
7. Munz B, Frank S, Hubner G, Olsen E, Werner S. A novel type of glutathione peroxidase: expression and regulation during wound repair. *Biochem J*. 1997;326 (Pt 2):579-585.

Table 1: Pool sizes of various metabolites in WT and myo$^{-/-}$ hearts after 25 min of perfusion with 5 mM glucose and 0.5 mM palmitate in the presence of 50 µU insulin. Data are means ± SD (n = 6, **P* < 0.05 vs WT).

Metabolite		**WT**	**myo$^{-/-}$**
Alanine	[mM]	1.93 ± 0.24	2.20 ± 0.41
Glutamate	[mM]	2.73 ± 0.37	2.86 ± 0.82
Lactate	[mM]	4.38 ± 1.97	4.81 ± 1.53
Taurine	[mM]	29.01 ± 2.26	29.20 ± 2.14

Table 2: Basal cardiac parameters of WT and myo$^{-/-}$ mice as assessed by MRI *in vivo*. The values are means ± SD (n=8).

Parameter		**WT**	***myo*$^{-/-}$**
Animal weight	[g]	41.4 ± 5.6	40.0 ± 3.8
Heart rate	[bpm]	483 ± 50	479 ± 39
Enddiastolic volume (EDV)	[µl]	104 ± 14	105 ± 14
Endsystolic volume (ESV)	[µl]	34.7 ± 8.9	38.8 ± 4.3
Stroke volume (SV)	[µl]	70.1 ± 6.7	66.1 ± 9.7
Ejection fraction (EF)	[%]	67.3 ± 5.4	62.3 ± 3.5
Cardiac output (CO)	[ml·min^{-1}]	34.1 ± 7.2	31.6 ± 6
Enddiastolic wall diameter	[mm]	0.97 ± 0.07	1.01 ± 0.09
Endsystolic wall diameter	[mm]	1.52 ± 0.06	1.52 ± 0.07
Systolic wall thickening	[%]	56.5 ± 7.9	51.5 ± 11.0
Left ventricular mass	[mg]	132 ± 14	138 ± 10
Heart body index	[mg·g^{-1}]	3.22 ± 0.31	3.45 ± 0.20

Table 3: Blood serum substrates of WT and myo$^{-/-}$ mice. The values are means ± SD (n=6).

Substrate			**WT**	**myo$^{-/-}$**
Glucose		[mg/dl]	212.3 ± 24.0	190.7 ± 42.3
Lactate		[mmol/l]	2.2 ± 0.2	1.5 ± 0.9
Palmitic acid	(16:0)	[mg/l]	1380.3 ± 449.8	1257.7 ± 534.8
Palmitoleic acid	(16:1)	[mg/l]	38.0 ± 13.1	36.0 ± 17.2
Stearic acid	(18:0)	[mg/l]	281.7 ± 40.0	305.0 ± 92.5
Oleic acid	(18:1)	[mg/l]	380.3 ± 65.4	399.0 ± 93.6
Arachidinic acid	(20:0)	[mg/l]	11.0 ± 6.5	13.3 ± 11.1
	(20:1)	[mg/l]	< 1	< 1
	(20:2)	[mg/l]	< 1	< 1
	(20:3)	[mg/l]	12.7 ± 12.5	19.0 ± 13.4
Arachidonic acid	(20:4)	[mg/l]	792.0 ± 67.5	859.0 ± 46.0

Table 4: Differentially expressed proteins in WT vs. myo$^{-/-}$ mice.

Spot	Identified protein	WT	myo$^{-/-}$	
	Down-regulated in myo$^{-/-}$	Spot volume [a.u.]		
572	Short-chain acyl-CoA dehydrogenase	182 ± 76	88 ± 57	*
156	Isovaleryl acyl-dehydrogenase	629 ± 129	327 ± 254	*
315	Short-chain enoyl-CoA hydratase I	157 ± 55	65 ± 47	**
316	Short-chain enoyl-CoA hydratase II	774 ± 217	521 ± 106	*
636	Electron transferring flavoprotein dehydrogenase	51 ± 35	10 ± 9	***
349	Apolipoprotein A1	193 ± 95	53 ± 35	**
399	α-(B)-Crystallin	925 ± 230	570 ± 157	**
343	Antioxidant protein 2 (123A)[#]	366 ± 118	0	***
385	Superoxide dismutase [Mn]	185 ± 60	58 ± 27	***
254	Voltage-dependent anion channel 1	324 ± 106	129 ± 54	***
111	Fumarate hydratase	602 ± 123	386 ± 118	**
	Up-regulated in myo-/-			
282	Glyceraldehyde 3-phosphate dehydrogenase	34 ± 12	178 ± 152	*
570	Trifunctional protein (α-fragment)	52 ± 61	370 ± 245	**
861	Trifunctional protein (α-fragment)	19 ± 14	112 ± 88	*
896	Trifunctional protein (α-fragment)	12 ± 10	101 ± 77	*
899	Trifunctional protein (α-fragment)	22 ± 24	340 ± 219	**
35	Mitochondrial stress-70 protein	195 ± 89	511 ± 263	*
908	Antioxidant protein 2 (123A → 123D) [#]	0	463 ± 171	***
292	ATP synthase α-chain (fragment)	189 ± 78	376 ± 175	*
387	ATP synthase α-chain (fragment)	15 ± 16	130 ± 102	*
483	Cardiac myosin heavy chain (fragment)	71 ± 33	223 ± 140	*

The annotation “fragment” indicates that the molecular weight of the protein on the gel is considerably smaller than that of the whole protein. indicates proteins involved in fatty acid metabolism and glycolysis, stress proteins, and other proteins. Data are means ± SD (n = 12, *P < 0.005, **P < 0.0005, ***P < 0.00005 vs. WT, respectively).

[#] Two different sequence variants of the antioxidant protein 2 are expressed in WT and myo$^{-/-}$ hearts, respectively.

FIGURE LEGENDS

Figure 1: Section of a ^{13}C NMR spectrum showing the glutamate C4 isotopomer pattern for a WT heart extract. Hearts were perfused for 25 min with 5 mM [1,6-$^{13}C_2$]glucose and 0.5 mM [U-$^{13}C_{16}$]palmitate in the presence of 50 µU insulin. Abbreviations: D34, doublet due to J_{34} coupling (34 Hz); D45, doublet due to J_{45} coupling (51 Hz); Q, quartet (doublet of doublet) due to J_{345} coupling (J_{34} 34 Hz, J_{45} 51 Hz); S, singlet.

Figure 2: Representative 2D-PAGE gels of WT and myo$^{-/-}$ hearts. Encircled spots are differentially expressed between the groups. For spot assignments and quantification refer to table 4.

Online data supplement

Figure 1

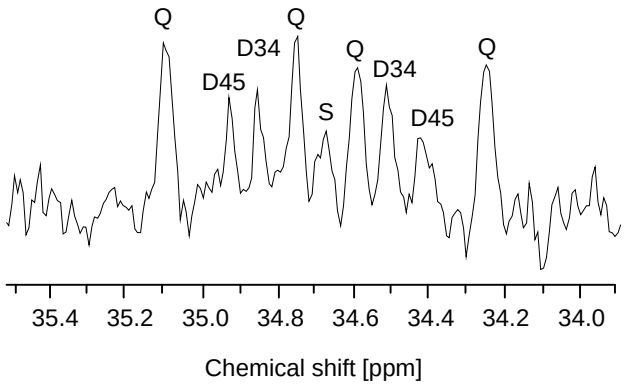

Online data supplement

Figure 2

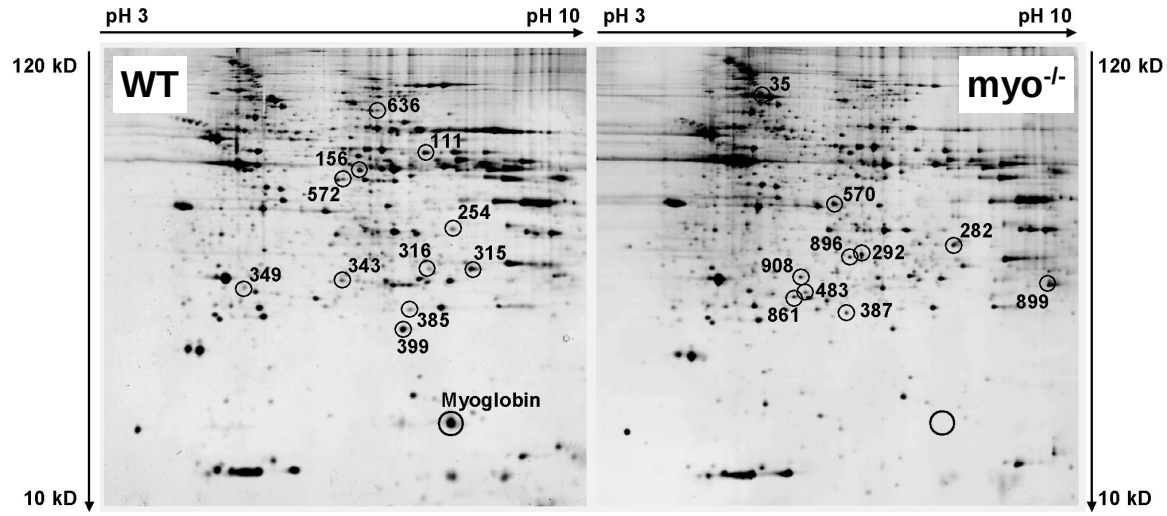

ONLINE DATA SUPPLEMENT

MATERIALS AND METHODS

Heart perfusion

General setup: Preparation of hearts and retrograde, non-recirculating perfusion at constant pressure of 100 mmHg with modified Krebs-Henseleit buffer – gassed at 95% O_2/5% CO_2 (carbogen), resulting in a pH of 7.4 – was performed essentially as described.[1] Perfusion pressure, coronary flow, and left ventricular developed pressure were measured continously. Signals were recorded with a sampling rate of 100 Hz utilizing a PC with dedicated software (ADInstruments, USA). Hearts were kept at 37 °C using a water-temperated glass jacket. After hearts had stabilized, cardiac pacing (500 bpm) was initiated and continued throughout. 30 minutes after onset of cardiac pacing, the coronary perfusion rate was fixed to the steady flow established and was maintained constant. Hearts were subsequently supplied with buffer which contained 5 mM glucose, 0.5 mM palmitate (bound to 3% albumin), and 50 µU insulin and was gassed at 95%O_2/5%CO_2 *via* a home-made bulb oxygenator.

Metabolic analysis: After hemodynamic and contractile parameters maintained constant under these conditions, hearts were finally switched to buffer containing 5 mM [1,6-$^{13}C_2$]glucose, 0.5 mM [U-$^{13}C_{16}$]palmitate (both from Cambridge Isotope Laboratories (Andover, USA), the latter bound to 3% essentially fatty acid free albumin), and 50 µU insulin. After 25 min of perfusion hearts were freeze-clamped, extracted with perchloric acid (PCA), neutralized, lyophilized, and stored at -20° C.

Measurement of myocardial oxygen consumption: Arterial and venous PO_2 were measured simultaneously with implantable oxygen micro-sensors based on 140 µm optical silica fiber

(Presens; Regensburg, Germany). For determination of arterial PO_2 one sensor was introduced *via* a branch connection into the perfusion line and positioned right in front of the aorta. Coronary venous PO_2 was measured by a second sensor which was advanced *via* the pulmonary artery into the right ventricle. Sensors were connected to a four-channel oxygen meter (OXY-4 micro) and signals were recorded continously with a sampling rate of 0.3 Hz by using a notebook with dedicated software (Presens, Regensburg, Germany). Oxygen consumption was calculated according to Fick's principle as the product of the arterio-venous O_2 content difference and coronary flow. Data were normalized for heart weights.

Magnetic resonance measurements

Data were recorded on a Bruker DRX 9.4 Tesla WB NMR spectrometer operating at frequencies of 400.1 MHz for ^{1}H measurements and 100.6 MHz for ^{13}C measurements.

Spectroscopy: Lyophilized PCA extracts were redissolved in 0.5 ml D_2O. Spectra were recorded from a 5-mm $^{1}H/^{13}C$ dual probe. ^{1}H NMR spectra were acquired with a flip angle of 90º, repetition time 15 s, low power water presaturation, 512 scans, spectral width 5580 Hz, data size 16 K, zero filling to 32 K. Chemical shifts were referenced to (trimethylsilyl)-propionic-2,2,3,3d_4-acid (TSP) at 0 ppm. For ^{13}C NMR spectra 20 K scans were accumulated with a flip angle of 30º, repetition time 1.7 s, composite pulse decoupling with Waltz16, spectral width 25062 Hz, data size 32 K, zero filling to 64 K, exponential weighting resulting in a 1 Hz line broadening. Chemical shifts were referenced to C3 of lactate at 21.3 ppm.

Imaging: Magnetic resonance imaging (MRI) was performed using a microimaging unit (Mini 0.5, Bruker) equipped with an actively shielded 57-mm gradient set (capable of

200 mT/m maximum gradient strength and 110 µs rise time at 100% gradient switching) and a 38-mm birdcage resonator. Mice were slightly anaesthetized with isoflurane (1.5%) and kept at 37° C. High resolution images of mice hearts were acquired using an electrocardiogram- and respiration-triggered fast gradient echo cine sequence with a flip angle < 30°, echo time < 2 ms, and a repetition rate of about 4 ms. The resulting in-plane resolution was 117·117 μm^2 (field of view 30·30 mm^2, 256·256 matrix, 1 mm slice thickness). The total acquisition time per slice for one cine sequence was about 2 min. Six to eight contiguous ventricular short axis slices were acquired to cover the entire heart.

Isotopomer analysis of carbon flow into the TCA cycle: The pool size of various metabolites has been determined from fully relaxed ^{1}H NMR spectra of extracts from hearts perfused with unlabelled substrates and are given in table 1 of this section. Quantitative evaluation of the spectra was done by using the mixed lorentzian/gaussian deconvolution availabe under X-WinNMR 2.6 (Bruker). The implemented automatic integration routine resulted in relative peak areas. TSP was used to standardize the concentration and integrated values were related to the protein content (Lowry) and converted to concentrations on the basis of a cytosolic water space of 4.3 µl/mg protein.[1] ^{13}C NMR spectra were corrected for natural abundant ^{13}C and were quantified as previously described.[2] The relative contributions of palmitate ($F_{Palmitate}$), glucose ($F_{Glucose}$), and endogenous sources ($F_{Endogenous}$) to the total acetyl-CoA pool entering the TCA cycle were determined from isotopomer analysis of glutamate carbons C3 and C4 only,[3] since S/N ratio of mouse heart ^{13}C NMR spectra was not sufficient to examine accurately glutamate carbon C2 in each case. Fluxes were calculated from the doublet due to J_{34} coupling (C4D34), the quartet or doublet of doublets (C4Q) due to J_{345} coupling (*cf.*

fig. 1), and the ratio of the total resonance areas of glutamate carbons C4 and C3 (C4/C3), *cf.* reference 3 for a detailed derivation of the following equations:

(1) $F_{Glucose} = (C4D34)/(C4/C3)$

(2) $F_{Palmitate} = (C4Q)/(C4/C3)$

(3) $F_{Endogenous} = 1 - F_{Glucose} - F_{Palmitate}$

Proteome analysis

Sample preparation and 2D-PAGE were essentially performed as previously reported.[4] In brief, following thoracotomy hearts were perfused *in situ* by phosphate-buffered saline, excised, weighted, and immediately lysed. After tissue homogenization and centrifugation at 14000 rpm (10 °C, 10 min) samples were divided into 50 µl aliquots and stored at -80 °C. For isoelectric focussing (IEF) immobilized pH gradients (IPGs) and the IPGphor system (Amersham Pharmacia Biotech) were used. Rehydration of IPG strips (24 cm, pH 3-10 linear gradient; containing 150 µg protein for analytical gels and up to 2 mg protein for preparative gels) and IEF were carried out as described.[2] SDS-PAGE was performed on a ETTAN-DALT II vertical electrophoresis unit (Amersham Pharmacia Biotech). Equilibrated IPG strips were placed on top of the gel (size of $0.1 \cdot 25.5 \cdot 20$ cm^3) and fixed in place by agarose sealing solution.[5] Twelve gels were run simultaneously (settings: 30 min, 30 W; 4.5 h, 180 W) and either silver-stained[6] or stained by coomassie blue R250.

Image analysis: The gels were digitized at 300 dpi, 8 bit gray scale, blue channel using a UMAX PowerLook III scanner calibrated by a photographic step tablet (Kodak). Images were

evaluated by the Image Master 2D Elite 3.10 software (Amersham Pharmacia Biotech). Background substraction was performed by the "mode of non spot" option (setting: 45 pixel). All spot volumes, *i.e.* spot area multiplied by the mean gray value, were divided by the sum of the volume of all spots detected on the gel. Faint spots (spot volume < 0.02 %) and doubtful spots (irreproducible, clustered or smeared) were excluded from the statistical analysis. A reference gel containing 583 valid spots was created from gels of 5 WT and 5 myo$^{-/-}$ samples and served as an index to the spots on individual gels.

RESULTS

Metabolite pool sizes

No differences were observed in pool sizes of metabolites (table 1) and fractional enrichments (data not shown) of alanine, glutamate, and lactate between WT and myo$^{-/-}$ hearts.

In vivo MRI analysis

Prior to PET analysis all mice were initially characterized by MRI which showed similar values for diastolic and systolic volumes as well as cardiac output in both groups (table 2).

Analysis of blood serum substrates

Both ^{13}C NMR and PET data indicate a shift to increased glucose and reduced fatty acid utilization transgenic hearts. To clarify whether these alterations may have been caused by differences in serum substrate concentrations, we determined the amounts of glucose, lactate, and various FAs (16:0, 16:1, 18:0, 18:1, 20:0, 20:1, 20:2, 20:3, 20:4) in WT and myo$^{-/-}$ mice (n=6). However, there were no significant differences between the two groups concerning all parameters analyzed (table 3).

Proteome analysis

Approximately 460 different protein species were recorded on each gel (fig. 2), with similar numbers of spots in both groups (466±18 in WT and 455±26, in myo$^{-/-}$, n=12 each). Besides Mb, 21 protein species were found to be differentially expressed when comparing myo$^{-/-}$ with WT samples (table 4): Eleven protein species showed decreased and 10 increased expression in myo$^{-/-}$ hearts. Noticeably, more than half of the proteins that were differentially expressed are involved in intermediary metabolism (table 4). Classification of the other altered proteins is less homogenous: five of them can be assigned to the group of stress proteins, whereas the remaining 5 proteins cannot be summed up under a common category. Ten of the 21 altered protein species are involved in FA metabolism (table 4). Nine of these are part of the mammalian mitochondrial β-oxidation pathway which are discussed in detail in the normal manuscript.

Further differentially expressed proteins (table 4 of this section lists all altered proteins determined by 2D-PAGE): Two chaperon related proteins were altered in expression: mitochondrial stress-70 protein (+160% in myo$^{-/-}$ vs. WT) and the α-subunit of (B)-crystallin (–38%). Furthermore, at unchanged expression level the antioxidant protein 2 (AOP2) showed a shift in the isoelectric point from pH 6.42 in WT to pH 6.05 in myo$^{-/-}$ mice. Sequence analysis of the proteins cDNA revealed alanine at position 123 to be replaced by asparagic acid in myo$^{-/-}$ hearts which can easily explain the shift in the isoelectric point. The same sequence variant of AOP2 has also been described elsewhere.[7] Mitochondrial manganese superoxide dismutase was found to be reduced by 69 % in myo$^{-/-}$ mice. Moreover, a prominent protein of the outer mitochondrial membrane, the voltage-dependent anion channel 1 was found to be decreased by 60% in Mb deficient hearts. Fumarate hydratase

which catalyses the dehydration of malate to fumarate exhibited less expression in myo$^{-/-}$ hearts, while other enzymes of the TCA cycle were not found to be differentially expressed. Additionally, we found that apolipoprotein A1 which is involved in serum lipid transport is reduced by 73% in hearts of Mb-deficient mice.

REFERENCES

1. Flögel U, Decking UK, Gödecke A, Schrader J. Contribution of NO to ischemia-reperfusion injury in the saline-perfused heart: a study in endothelial NO synthase knockout mice. *J Mol Cell Cardiol*. 1999;31:827-836.
2. Flögel U, Willker W, Leibfritz D. Determination of de novo synthesized amino acids in cellular proteins revisited by ^{13}C NMR spectroscopy. *NMR Biomed*. 1997;10:50-58.
3. Malloy CR, Thompson JR, Jeffrey FM, Sherry AD. Contribution of exogenous substrates to acetyl coenzyme A: measurement by ^{13}C NMR under non-steady-state conditions. *Biochemistry*. 1990;29:6756-6761.
4. Laussmann T, Janosi RA, Fingas CD, Schlieper GR, Schlack W, Schrader J, Decking UK. Myocardial proteome analysis reveals reduced NOS inhibition and enhanced glycolytic capacity in areas of low local blood flow. *FASEB J*. 2002;16:628-630.
5. Li Y, Huang TT, Carlson EJ, Melov S, Ursell PC, Olson JL, Noble LJ, Yoshimura MP, Berger C, Chan PH, . Dilated cardiomyopathy and neonatal lethality in mutant mice lacking manganese superoxide dismutase. *Nat Genet*. 1995;11:376-381.
6. Blum H, Gross HJ, Beier H. Improved silver staining of plant proteins, RNA and DNA in polyacrylamide gels. *Electrophoresis*. 1987;8:83-89.
7. Munz B, Frank S, Hubner G, Olsen E, Werner S. A novel type of glutathione peroxidase: expression and regulation during wound repair. *Biochem J*. 1997;326 (Pt 2):579-585.

Table 1: Pool sizes of various metabolites in WT and myo$^{-/-}$ hearts after 25 min of perfusion with 5 mM glucose and 0.5 mM palmitate in the presence of 50 µU insulin. Data are means ± SD (n = 6, **P* < 0.05 vs WT).

Metabolite		**WT**	**myo$^{-/-}$**
Alanine	[mM]	1.93 ± 0.24	2.20 ± 0.41
Glutamate	[mM]	2.73 ± 0.37	2.86 ± 0.82
Lactate	[mM]	4.38 ± 1.97	4.81 ± 1.53
Taurine	[mM]	29.01 ± 2.26	29.20 ± 2.14

Table 2: Basal cardiac parameters of WT and myo$^{-/-}$ mice as assessed by MRI *in vivo*. The values are means ± SD (n=8).

Parameter		**WT**	***myo*$^{-/-}$**
Animal weight	[g]	41.4 ± 5.6	40.0 ± 3.8
Heart rate	[bpm]	483 ± 50	479 ± 39
Enddiastolic volume (EDV)	[µl]	104 ± 14	105 ± 14
Endsystolic volume (ESV)	[µl]	34.7 ± 8.9	38.8 ± 4.3
Stroke volume (SV)	[µl]	70.1 ± 6.7	66.1 ± 9.7
Ejection fraction (EF)	[%]	67.3 ± 5.4	62.3 ± 3.5
Cardiac output (CO)	[ml·min^{-1}]	34.1 ± 7.2	31.6 ± 6
Enddiastolic wall diameter	[mm]	0.97 ± 0.07	1.01 ± 0.09
Endsystolic wall diameter	[mm]	1.52 ± 0.06	1.52 ± 0.07
Systolic wall thickening	[%]	56.5 ± 7.9	51.5 ± 11.0
Left ventricular mass	[mg]	132 ± 14	138 ± 10
Heart body index	[mg·g^{-1}]	3.22 ± 0.31	3.45 ± 0.20

Table 3: Blood serum substrates of WT and myo$^{-/-}$ mice. The values are means ± SD (n=6).

Substrate			**WT**	**myo$^{-/-}$**
Glucose		[mg/dl]	212.3 ± 24.0	190.7 ± 42.3
Lactate		[mmol/l]	2.2 ± 0.2	1.5 ± 0.9
Palmitic acid	(16:0)	[mg/l]	1380.3 ± 449.8	1257.7 ± 534.8
Palmitoleic acid	(16:1)	[mg/l]	38.0 ± 13.1	36.0 ± 17.2
Stearic acid	(18:0)	[mg/l]	281.7 ± 40.0	305.0 ± 92.5
Oleic acid	(18:1)	[mg/l]	380.3 ± 65.4	399.0 ± 93.6
Arachidinic acid	(20:0)	[mg/l]	11.0 ± 6.5	13.3 ± 11.1
	(20:1)	[mg/l]	< 1	< 1
	(20:2)	[mg/l]	< 1	< 1
	(20:3)	[mg/l]	12.7 ± 12.5	19.0 ± 13.4
Arachidonic acid	(20:4)	[mg/l]	792.0 ± 67.5	859.0 ± 46.0

Table 4: Differentially expressed proteins in WT vs. myo$^{-/-}$ mice.

Spot	Identified protein	WT	myo$^{-/-}$	
	Down-regulated in myo$^{-/-}$	Spot volume [a.u.]		
572	Short-chain acyl-CoA dehydrogenase	182 ± 76	88 ± 57	*
156	Isovaleryl acyl-dehydrogenase	629 ± 129	327 ± 254	*
315	Short-chain enoyl-CoA hydratase I	157 ± 55	65 ± 47	**
316	Short-chain enoyl-CoA hydratase II	774 ± 217	521 ± 106	*
636	Electron transferring flavoprotein dehydrogenase	51 ± 35	10 ± 9	***
349	Apolipoprotein A1	193 ± 95	53 ± 35	**
399	α-(B)-Crystallin	925 ± 230	570 ± 157	**
343	Antioxidant protein 2 (123A)[#]	366 ± 118	0	***
385	Superoxide dismutase [Mn]	185 ± 60	58 ± 27	***
254	Voltage-dependent anion channel 1	324 ± 106	129 ± 54	***
111	Fumarate hydratase	602 ± 123	386 ± 118	**
	Up-regulated in myo-/-			
282	Glyceraldehyde 3-phosphate dehydrogenase	34 ± 12	178 ± 152	*
570	Trifunctional protein (α-fragment)	52 ± 61	370 ± 245	**
861	Trifunctional protein (α-fragment)	19 ± 14	112 ± 88	*
896	Trifunctional protein (α-fragment)	12 ± 10	101 ± 77	*
899	Trifunctional protein (α-fragment)	22 ± 24	340 ± 219	**
35	Mitochondrial stress-70 protein	195 ± 89	511 ± 263	*
908	Antioxidant protein 2 (123A → 123D) [#]	0	463 ± 171	***
292	ATP synthase α-chain (fragment)	189 ± 78	376 ± 175	*
387	ATP synthase α-chain (fragment)	15 ± 16	130 ± 102	*
483	Cardiac myosin heavy chain (fragment)	71 ± 33	223 ± 140	*

The annotation “fragment” indicates that the molecular weight of the protein on the gel is considerably smaller than that of the whole protein. indicates proteins involved in fatty acid metabolism and glycolysis, stress proteins, and other proteins. Data are means ± SD (n = 12, *P < 0.005, **P < 0.0005, ***P < 0.00005 vs. WT, respectively).

[#] Two different sequence variants of the antioxidant protein 2 are expressed in WT and myo$^{-/-}$ hearts, respectively.

FIGURE LEGENDS

Figure 1: Section of a ^{13}C NMR spectrum showing the glutamate C4 isotopomer pattern for a WT heart extract. Hearts were perfused for 25 min with 5 mM [1,6-$^{13}C_2$]glucose and 0.5 mM [U-$^{13}C_{16}$]palmitate in the presence of 50 µU insulin. Abbreviations: D34, doublet due to J_{34} coupling (34 Hz); D45, doublet due to J_{45} coupling (51 Hz); Q, quartet (doublet of doublet) due to J_{345} coupling (J_{34} 34 Hz, J_{45} 51 Hz); S, singlet.

Figure 2: Representative 2D-PAGE gels of WT and myo$^{-/-}$ hearts. Encircled spots are differentially expressed between the groups. For spot assignments and quantification refer to table 4.

Online data supplement

Figure 1

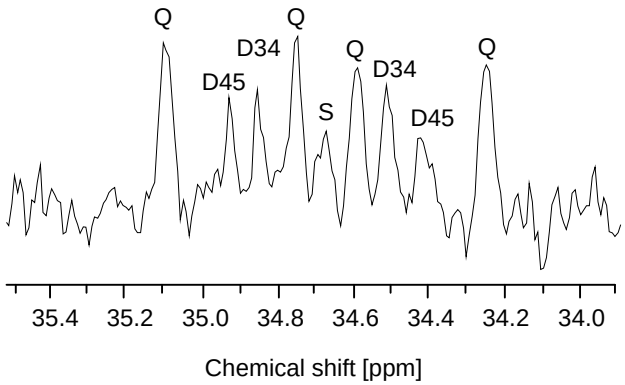

Online data supplement

Figure 2